

SELF ABSORPTION IN PLASMAS

By
GEORGE ROBERT SHIPMAN

A THESIS PRESENTED TO THE GRADUATE COUNCIL OF
THE UNIVERSITY OF FLORIDA
IN PARTIAL FULFILLMENT OF THE REQUIREMENTS FOR THE
DEGREE OF MASTER OF SCIENCE

UNIVERSITY OF FLORIDA
1968

DEDICATION

To Dr. Ray Hefferlin

Who showed me that everything
in the universe is a special
case of the spectrograph.

ACKNOWLEDGEMENTS

My gratitude is expressed, first and foremost to Dr. Ray Hefferlin who suggested the thesis topic, inspired and encouraged my efforts, supplied the data in Section V, and was both a teacher and a friend.

Next I am indebted to my chairman, Dr. K-Y Chen for patience, understanding, and helpful discussions of stellar plasmas. The help and encouragement of Dr. R. T. Schneider, particularly toward understanding nonequilibrium plasmas, is gratefully acknowledged.

I appreciate the financial support of the Department of Physics and Astronomy during my first year of graduate study, and the support of its chairman, Dr. S. S. Ballard, which made my efforts possible.

Last, I wish to thank Dr. T. L. Bailey and Dr. Guy Omer who served on my committee and from whom I have learned much, both in and outside the classroom, Mr. W. W. Richardson who drew two of the graphs, and Mrs. J. M. Davis who uncomplainingly typed from an often illegible manuscript.

PREFACE

This paper is motivated by a desire to know a priori if any given spectrum line in any given source under any given excitation condition is self absorbed and, if so, by how much is the observed intensity less than that which would be observed in the optically thin case.

TABLE OF CONTENTS

	Page
Acknowledgements	iii
Preface.	iv
List of Tables	vi
List of Figures	vii
Abstract	viii
Section	
I. What is Self Absorption.	1
II. The Effects of Self Absorption	4
III. Tests for and Indications of Self Absorption	7
IV. Using Self Absorption to Determine Abundance and Line Shape Parameter a	25
V. Experimental Determinations of Self Absorption in a Plasma Jet	33
Glossary	45
Appendix I	49
Appendix II	50
Appendix III	53
Bibliography	55
Biographical Sketch	58

LIST OF TABLES

Table	Page
I. Details of Calculations for Self Reversal Parameter p , at $Z = 0$	38
II. Details of the Calculations to Compare Line Center Specific Intensity with Planck Function at Same Wavelength. Lines Selected were the Most Intense and/or Illustrated Typical Lines in a Given Spectral Region. $Z = 0$	40
III. Details of Calculations for Self Reversal Parameter p , at $Z = 1''$	41
IV. Details of the Calculations to Compare Line Center Specific Intensity with Planck Function at same Wavelength. Lines Selected were the most Intense and/or Illustrated Typical Lines in a given Spectral Region. $Z = 1''$	42
V. Spectral Line Intensities ($\text{ergs sec}^{-1} \text{ster}^{-1} \text{cm}^{-2}$).	43

LIST OF FIGURES

Figure	Page
1 Spectrochemical Working Curves	8
2 Effect of Self Absorption on Line Profile	17
3 Reversal Curve for Resonance Line Shape	18
4 Reversal Curve for Doppler Line Shape	19
5 Reversal Curve under Different Conditions of Line Shape and Measurement	20
6 Curve of Growth	27
7 Theoretic Duplication Curves	28
8 Graphical Interpolation of Duplication Curve with Curve of Growth	31
9 Plasma Jet	34
10 Boltzmann Plot	35

SECTION I

WHAT IS SELF ABSORPTION

When light emitted by an atom at some point in a light source is absorbed by the same kind of atom at some other point in that light source, the source is said to exhibit self absorption.

There exists a great deal of divergence between the terminology used by plasma physicists studying laboratory plasmas and astrophysicists studying stellar plasmas.^{(15) (16)}

When a plasma spectroscopist speaks of self absorption or radiation trapping, he is referring to any process by which a photon emitted by an atom of species A interior to the boundary of the excited plasma is prevented from leaving the plasma by another atom of species A. Included are those processes which astrophysicists call:^{(4) (3)}

- "true selective absorption" an atom absorbs a photon of energy $h\nu$, becomes excited and subsequently undergoes a radiationless transition (super-elastic collision) thus decreasing the energy of the radiation field in units of $h\nu$.
- "coherent scattering" an atom absorbs a photon of energy $h\nu$, and subsequently undergoes a radiative transition, emitting a photon of energy $h\nu$ either in a random direction (isotropic scattering) or in some preferred direction (anisotropic scattering).

"noncoherent scattering" an atom absorbs a photon of energy $h\nu$ and subsequently emits a photon of some other energy $h\nu'$. The excess excitation energy may be lost either through emission of other photons (cascading) or through electron collisions.

If all the photons of energy $h\nu$ produced by a source emerge from the source, the source is said to be optically thin at that frequency. Another way of saying the same thing is that the local radiative intensity does not affect the equations of statistical equilibrium and the statistical state of the gas does not affect the local radiation field. The foregoing implies that the equations of statistical equilibrium and the radiative transfer equation are decoupled.⁽⁶⁾ If none of the photons of energy $h\nu$ emerge from the source, the source is said to be optically thick at the frequency ν . The foregoing is equivalent to saying that the radiation field at a point is fixed by only the local value of the source function.⁽⁶⁾ Where the source is optically thick for all ν , it is said to be in "local thermal equilibrium" (LTE), and the emergent flux is closely approximated by the Planck radiation law. Again the equations of statistical equilibrium and the equation of radiative transfer are decoupled.⁽²⁵⁾

One may expect self absorption to occur more easily for certain types of geometries than for others. For instance, in any source where the number of atoms in the ground state increases with distance from the center either because the actual density increases or because the temperature decreases, the possibility of self absorption is great.⁽¹¹⁾

Any spectroscopic determination of any physical characteristic of any excited plasma requires a knowledge of the "true" light intensity,

i.e. that intensity which would be observed if there were no self absorption. Stated another way, to use an optically thin model one must know what fraction of the photons of a given energy emitted in the solid angle subtended by the spectrographic optics do not reach the detector.

The spectroscopist can rather easily handle the two extreme cases:

- 1) optically thin LTE plasmas where all the photons reach the detector.
- 2) optically thick LTE plasmas where none of the photons reach the detector (as this case would not be visible,⁽⁷⁾ in practice it is assumed that the amount of energy leaving the plasma as radiation does not change the energy distribution in the plasma).

In general, a plasma will be optically thin at some wavelengths and optically thick at others. The intensity at in case 1) will be given by

$$I = N_{\nu} h\nu A_{\nu\lambda}$$

The intensity in case 2) will be approximated by the Planck radiation law.

The problem of determining the degree of self absorption is usually circumvented by studying the plasma at a wavelength which is known to be optically thin.⁽³¹⁾ There exists a slight ambiguity in the nomenclature and often a wavelength at which the plasma is optically thin is referred to as itself optically thin, i.e. an optically thin line.

The number of photons which do not reach the detector is clearly a function of density (or pressure), for as the number of particles between the radiating atom and the spectrograph is increased, the probability that the photon will be reabsorbed and re-emitted in another direction also increases.

SECTION II

THE EFFECTS OF SELF ABSORPTION

The most deleterious effect of self absorption is to cause departures from the optically thin model, thereby invalidating the use of the equation $I = N_u h \nu A_{ul}$ for calculating the emergent intensity, I . Thus, if there is significant coupling between the equations of statistical equilibrium and the equation of radiative transfer it is possible for the radiation field to effect changes in the energy density distribution of the plasma.⁽⁶⁾ This may be seen by observing that the rate equations governing the excited state densities contain the three radiative transition probabilities, two of which depend on the local intensity of the radiation field. This coupling is often large for astrophysical sources due to the high intensity of the radiation field whereas in laboratory plasmas it is usually necessary to consider the coupling only for resonance radiation and even then only for plasmas with significant optical depth.^{(10) (13)}

The most basic and most easily understood model for a plasma (and also the one most likely to be in equilibrium) is the thermal or collision dominated plasma. In this model, each excitation or ionization is caused by collisions and each de-excitation is by a super elastic collision or three-body recombination.⁽¹⁴⁾ Since the mass of the electron is so much smaller than that of any other specie in the plasma, they have very high velocities compared to the ions and neutral atoms. Also because it is the velocity of the colliding particle rather than

the momentum which results in the excitation and, in addition, electron reaction cross-sections are of the same order of magnitude as those of the ions, it is electron collisions which dominate the reaction rates.⁽⁵⁾ The electrons may be expected to have a Maxwellian velocity distribution since no mechanism has been found which can support a steady state non-Maxwellian distribution.⁽⁵³⁾ (36) (9) (61)

This model, however, fails to explain the mechanism by which the plasma emits radiation. It must be assumed then that there does exist some spontaneous radiative decay. The cross sections for radiative de-excitation are much larger than those of radiative excitation so that the net effect of radiation is to upset the equilibrium energy distribution. Detailed balancing no longer exists. In addition, since collisional excitation cross-sections increase with increasing principal quantum number whereas radiative de-excitation cross sections decrease, the energy loss is selectively from those states of lower energy. Thus we find that LTE relations hold only for levels above the point at which radiative de-excitation may be neglected compared to collisional de-excitation.⁽⁵⁾ What now is the effect of self absorption on this energy balance? It should be noted that what has happened is that detailed balancing no longer obtains, for while collisional excitation and collisional de-excitation are exact inverses, we have considered no inverse for radiative de-excitation. Self absorption supplies this inverse.⁽³⁰⁾ As the optical depth of the plasma increases, an increasing amount of the radiation is trapped within the plasma and results in radiative excitation, thus helping to restore the equilibrium energy balance.⁽³²⁾

A very important problem exists in the analysis of radiation from sources where significant departures from LTE may be expected (such as the solar chromosphere) namely, how can effects due to self absorption

be separated from those caused by departures from LTE? Both phenomena cause the emitted intensity to be less than that observed from an optically thin, LTE plasma; in the first case because some of the photons are trapped in the plasma, and in the second because the upper levels are underpopulated compared with a Maxwell-Boltzmann population distribution. Thomas and Athay⁽⁶⁾ have provided a partial solution to the problem for the case of the solar chromosphere by making observations of line profiles at various heights. This allows them to examine the variation of occupation number and source function with height and optical depth. (21) (28) (29) (18) (19) (20) (22) (23) (24)

SECTION III

TESTS FOR AND INDICATIONS OF SELF ABSORPTION

There exist several ways that one may test for the existence of self absorption. In the most general sense, "Any diagnostic technique that assumes optical thinness yields to the extent that it gives correct answers, a posteriori evidence of optical thinness."⁽⁵⁸⁾

One of the most powerful techniques is to determine experimentally how the intensity of some spectrum line varies with the number of emitters. This variation, I as a function of N , is plotted in some standard form and compared to a theoretic plot of the same quantities in which self absorption is neglected. Deviations between the two curves will serve to indicate self absorption. Several forms of this basic relation occur in the literature.

The Working Curve

What is perhaps the most straightforward approach to the problem is the "working curve" developed by the analytic spectrochemists.^{(1) (2)} In the simplest case, this is just a plot of the logarithm of intensity (on a relative scale) vs. the logarithm of the concentration (usually in parts per million) obtained by observing a set of standards with known concentrations. Often however, to reduce errors due to source fluctuation and variation of excitation conditions, the following variation is plotted (Figure 1)

Here on a log-log scale is the ratio of the intensity of the line under consideration to a line of the matrix which has about the same

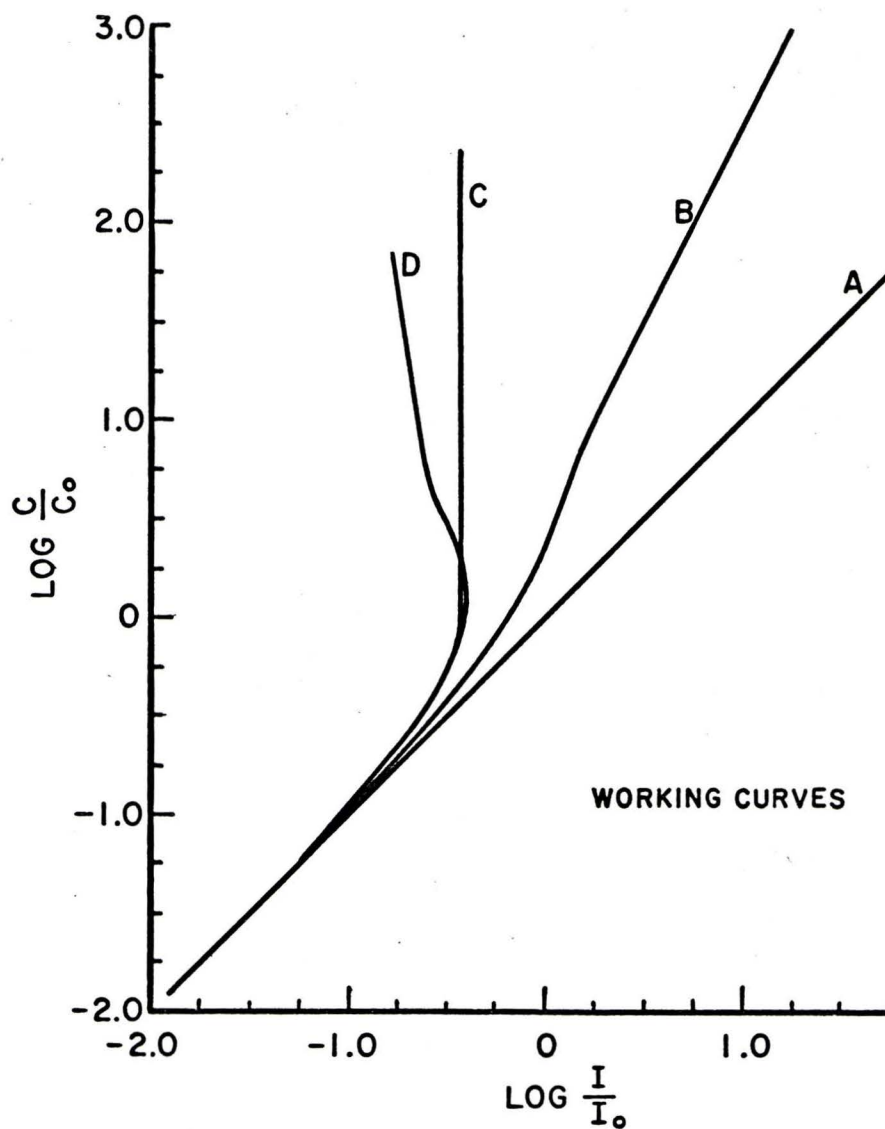


Figure 1. Spectrochemical working curves under various conditions of self absorption. A: no self absorption. B: resonance shape. C: line maxima measured. D: Doppler shape, total intensity measured (after 55).

excitation characteristics I/I_0 (same upper and lower excitation potentials, same transition probability, same statistical weight) vs. the assumed known ratio of concentrations c/c_0 . Once a curve of this form has been plotted from a set of standards, the intensity of the line due to the unknown is measured and hence the concentration is determined. By comparing this curve with theoretical curves for various source models and line profiles, the amount of self absorption in the source may be determined.

Ideally (i.e. for the optically thin case) the curve will be a straight line with a slope of 1 indicating a linear variation between the number of atoms and the intensity. For small values of density this is the case. However, as the density increases the amount of self absorption increases and the curve deviates from a straight line.

This method is not very useful for the astronomer or plasma spectroscopist for in general he will not have readily available a nice set of standards(!). In addition, a curve of this kind must be drawn for each line under consideration which is a tedious and laborious task for a spectrum with the complexity of, say, iron. This method is inconvenient from another standpoint, i.e. it is a posteriori. If it is necessary to know whether or not the 3100A iron line is self absorbed for a given temperature and density, it is necessary to go into the laboratory and perform an experiment before the answer can be determined.

The Curve of Growth

A more sophisticated version of the working curve is the "curve of growth." It is possible to plot a curve of growth using the intensities of either an emission line or an absorption line.

For the case of emission lines, consider the equation of radiative transport:

$$\frac{dI_\nu}{d\tau_\nu} = J_\nu(\tau) - I_\nu$$

Where I_ν is the specific intensity of the spectrum line and where $J_\nu(\tau)$ is the source function. If the source is assumed to be in LTE then it has a "true absorption" atmosphere rather than a scattering atmosphere and $J_\nu(\tau)$ may be replaced by $B_\nu(\tau)$ the Planck function. Thus:

$$\frac{dI_\nu}{d\tau_\nu} = B_\nu - I_\nu$$

the formal solution of which is

$$I_\nu = B_\nu(1 - e^{-\tau_\nu})$$

The total power radiated in a spectrum line is then

$$I = \int_{\text{line}} B_\nu(1 - e^{-\tau_\nu}) d\nu$$

Assuming that B_ν does not vary over the line

$$I = B_\nu \int_{\text{line}} (1 - e^{-\tau_\nu}) d\nu$$

For small values of τ_ν , we may expand the exponential term giving

$$I/B_\nu \doteq \int_{\text{line}} \tau_\nu d\nu$$

by the definition of τ_ν

$$\tau_\nu = k_\nu n_l l$$

$$I/B_\nu \doteq l n_l \int_{\text{line}} k_\nu d\nu$$

$$= l n_0 g_l e^{-E_\nu/kT_e} \frac{\pi e^2}{m c} f_{lu}$$

Hence for small values of τ_ν , I/B_ν should vary linearly with abundance, n_0 . Deviations from linearity indicate self absorption. For large

values of τ_ν , the form of the curve is dependent on the line shape parameter a .

In the case of absorption lines, a quantity is defined called the equivalent width. (44) (45) (49) (50) (51)

$$\begin{aligned} W_\nu &= \int \frac{I_0 - I_\nu}{I_0} d\nu \\ &= \int \left(1 - \frac{I_\nu}{I_0}\right) d\nu \end{aligned}$$

Using Beer's law,

$$W_\nu = \int (1 - e^{-\tau_\nu}) d\nu .$$

The equivalent width is plotted against some function of (nfl) , the optical depth.

The form of this result suggests a relationship between W_ν and I/B_ν . (54) What this relationship is may be seen by considering Kirchoff's law. (33)

$$\begin{aligned} I &= I_0 (\nu_0, T) A \\ &= I_0 (\nu_0, T) \int_{\text{line}} A_\nu d\nu \\ &= I_0 (\nu_0, T) \int_{\text{line}} (1 - e^{-\tau_\nu}) d\nu . \end{aligned}$$

Here, $A(\nu)$ is the absorptivity of the source at ν . The integrated absorptivity is just the equivalent width, hence the intensity and equivalent width are related through the Planck function and a measurement of either one will yield the other. Thus a curve of growth can be

constructed using either expression. ⁽³⁴⁾ ⁽³⁵⁾ For most laboratory plasmas it is more convenient to measure intensity (with the exception of flames where it is possible to use a continuous background source to produce absorption lines).

We will return to the curve of growth in the next section where examples will be given and it will be shown how to use the curve to determine certain physical parameters of the plasma.

The Duplication Curve

The duplication curve is a relation which has been used almost exclusively by groups studying flames ⁽⁵⁶⁾ though arc work ⁽⁴²⁾ has been done. The basic idea behind this method is the following; a mirror is placed behind the source which serves to focus the light received in a solid angle Ω back onto the source. In the optically thin case with allowance made for the reflectance of the mirror at the wavelength under consideration, twice as much light will reach the spectrograph when the mirror is used. Let I_1 be the intensity without the mirror in the system and I_2 be the intensity with the mirror. Define a quantity,

$$D = \frac{I_2 - I_1}{I_1}$$

As γ_v approaches infinite (optically thick case), D tends to zero while for $\gamma_v = 0$ (optically thin), D approaches 1. D is then plotted against some function of the concentration. This curve is the duplication curve. For large values of γ_v , the form of the curve varies according to the line shape parameter a . It should be noted that the duplication curve is just the derivative of the curve of growth.

When using this method, the reflectance of the mirror at the wavelength under consideration must be carefully measured. In addition, if

spacially resolved measurements are being attempted it is necessary to reinvert the image of the source in order to obtain correct orientation. (42) Of course, all optical elements used to effect the inversion must have their reflectance or transmission properties measured at the wavelength under consideration.

If the duplication factor D is known in absolute measure, the relative loss in emission due to self absorption $\frac{\hat{I}_\nu - 1}{\hat{I}_\nu}$, where \hat{I}_ν is the relative intensity normalized to the value of the Planck function at the same ν and T , may be determined by $(\hat{I}_\nu - 1) = \frac{1}{2}(1 - D)$ if $(\hat{I}_\nu - 1)$ is small compared to unity. (57) As long as $(\hat{I}_\nu - 1) \leq 0.1$ this relation does not depend noticeably on the line shape parameter a .

It is to be noted that in inhomogeneous sources into which class most laboratory plasmas fall (arcs, plasma jets, etc.) where the excitation may be crudely described by a two-zone model with a high excitation "filament" surrounded by a lower excitation "atmosphere" the optical path is really increased by a factor of three. Photons produced in the high excitation core must traverse the atmosphere (reversing layer) once to reach the spectrograph directly whereas the photons reflected from the mirror must pass through the cooler atmosphere three times.

We will return to the duplication curve in Section IV where examples will be given and it will be shown how the curve may be used to determine certain physical parameters of the plasma.

The Reversal Curve

Another curve which is of the same general form is the "reversal curve." (55) Consider a spectrum line with center frequency ν_0 and

an intensity distribution within the line given by ρ_ν i.e. ρ_ν is the radiation density. The absorption in a given thickness is proportional to ρ_ν , n_L , the number of atoms capable of absorbing the radiation of frequency ν , the properties of the individual atom and the interactions of that atom with the surrounding particles. We may write

$$1 \quad \frac{d\rho_\nu}{dx} = -k R_a(\nu, x) \rho_\nu$$

where $R_a(\nu, x)$ is a distribution function representing the number of photons absorbed at each frequency ν at each position x within the source, i.e. the absorption profile. $R_a(\nu, x)$ is normalized, for all x .

$$\int_{\text{LINE}} R_a(\nu, x) d\nu = 1 .$$

It can be shown that (Appendix I)

$$k = \frac{h\nu_0 B_{L\nu}}{c} n_L(x) .$$

Thus from 1) we have

$$\frac{d\rho_\nu}{\rho_\nu} = - \frac{h\nu_0 B_{L\nu}}{c} n_L(x) R_a(\nu, x) dx .$$

Integrating gives

$$\rho_\nu(r) = \rho_\nu(r_0) \exp\left[- \frac{h\nu_0 B_{L\nu}}{c} \int_{r_0}^r n_L(x) R_a(\nu, x) dx\right] .$$

The above is the plane wave solution. To deal with spherical waves produced by a point source, $\rho_\nu(r_0)$ must be replaced by $\rho_0(\nu, r)$ giving

$$P_\nu(r) = P_\nu(\nu, r) \exp\left[-\frac{h\nu_0 B_{L\nu}}{c} \int_{r_0}^r n_L(x) P_a(\nu, x) dx\right].$$

Considering a normalized emission distribution function, the above may be written in terms of intensities such that the intensity at r is

$$I_\nu(r) = I_0 P_e(\nu, r_0) \exp\left[-\frac{h\nu_0 B_{L\nu}}{c} \int_{r_0}^r n_L(x) P_a(\nu, x) dx\right]$$

Under certain conditions⁽³¹⁾ (8) (7) we may assume that

$$P_e(\nu, x) = P_a(\nu, x) = P(\nu, x)$$

i.e. the shapes of the emission and absorption lines are the same.

For simplicity assume $P(\nu, x)$ is independent of x and may be written P_ν . Cowan and Dieke⁽⁵⁵⁾ define a quantity p

$$p = \frac{h\nu_0 B_{L\nu}}{c} P_\nu \int n_L(x) dx,$$

in terms of which equation 2) may be written

$$I_\nu = I_0 P_\nu \exp\left[-p \frac{P_\nu}{P_{\nu_0}}\right].$$

For the case of no absorption, $p = 0$ and I_ν assumes the form of the distribution (shape) function P_ν .

More general expressions may be derived for the intensity of a line of arbitrary shape in any given source model (Appendix III). If it were possible to know a priori the shape of a given line and its p value, it would then be a simple matter to correct the observed intensities for self absorption and get the unabsorbed (optically thin) intensity. To see how critically the line intensity depends on the

ρ value it is instructive to plot I_ν vs. ν for various values of ρ assuming a natural dispersion profile (Figure 2).

It is evident that $\rho > 1$ corresponds to self reversal. It is also distressingly evident that the line profile for $\rho = 0.5$ which gives an intensity reduction of about forty percent could hardly be distinguished from the shape of a line with no self absorption. In an attempt to provide a workable expression for ρ , Hefferlin⁽⁵⁴⁾ (Appendix II) has derived for the resonance line shape

$$\rho = \frac{e^2}{mc} \frac{1}{\Delta\nu} \frac{g_u f_{ul}}{U(T)} N_e \exp\left[-\frac{E_L}{kT_e}\right].$$

This expression has been tested (Section V) with rather disappointing results. The calculated value of ρ tends to be drastically overconservative. A possible cause of the disparity is a poor choice of source model. Hefferlin⁽¹⁷⁾ is working on a more sophisticated source model which may clear up many of the points of divergence.

Extensive work has been done, mainly by the Russians^{(38) (39) (40) (41) (43) (46) (48)} comparing the models of Cowan and Dieke⁽⁵⁵⁾ with various laboratory sources. This work seems to indicate the necessity of constructing more sophisticated source models (model atmospheres).⁽¹²⁾ Much can be learned from the astrophysicists along these lines. One may now draw a "reversal curve" by plotting $\log I/I_0$ versus $\log \rho$ for various source models and line profiles (Figure 3, Figure 4, Figure 5).

Line Profile

The simplest (but by no means the most reliable) method for determining if an emission line is affected by self absorption is to examine the profile of the line. In cases of extreme self absorption the lines

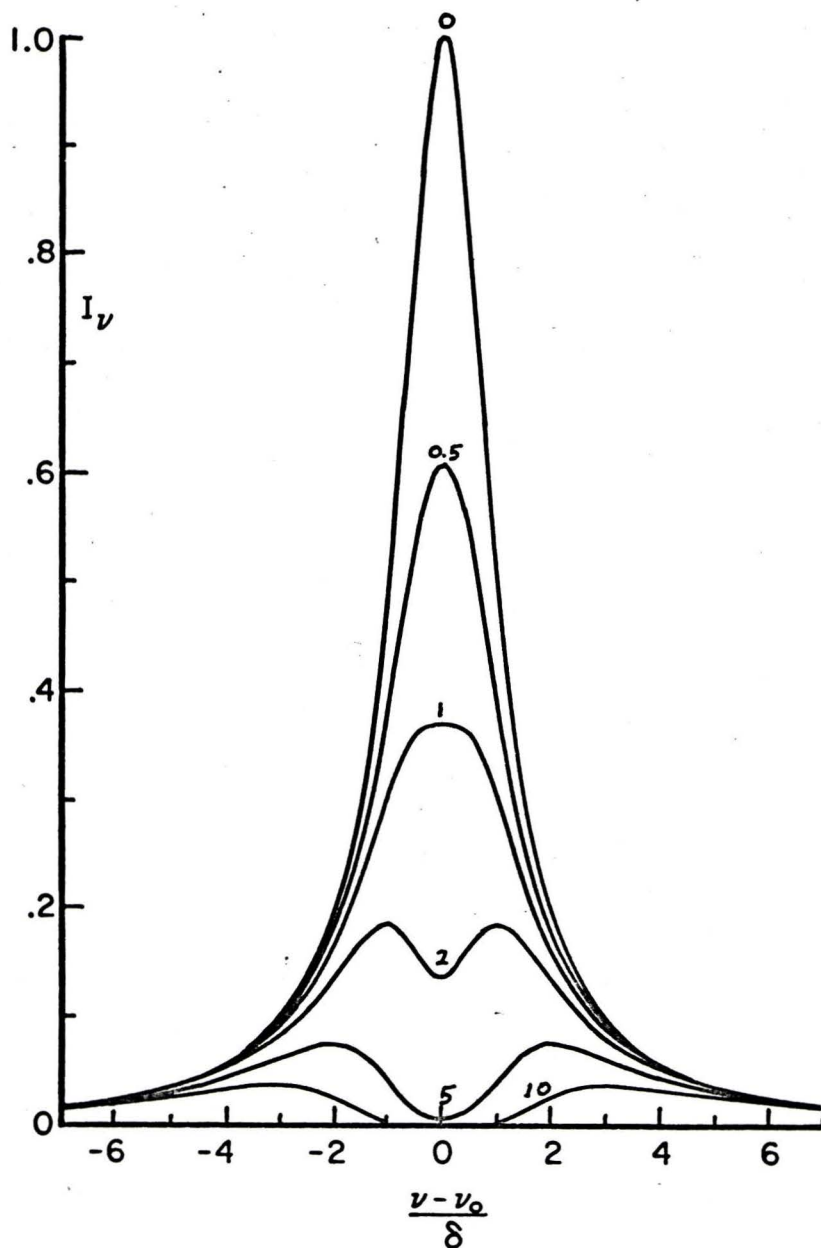


Figure 2. Line shapes with varying degree of self absorption as expressed by the absorption parameter p . The lines are plotted so that the unabsorbed line in each case would have the shape shown for $p = 0$ (after 55).

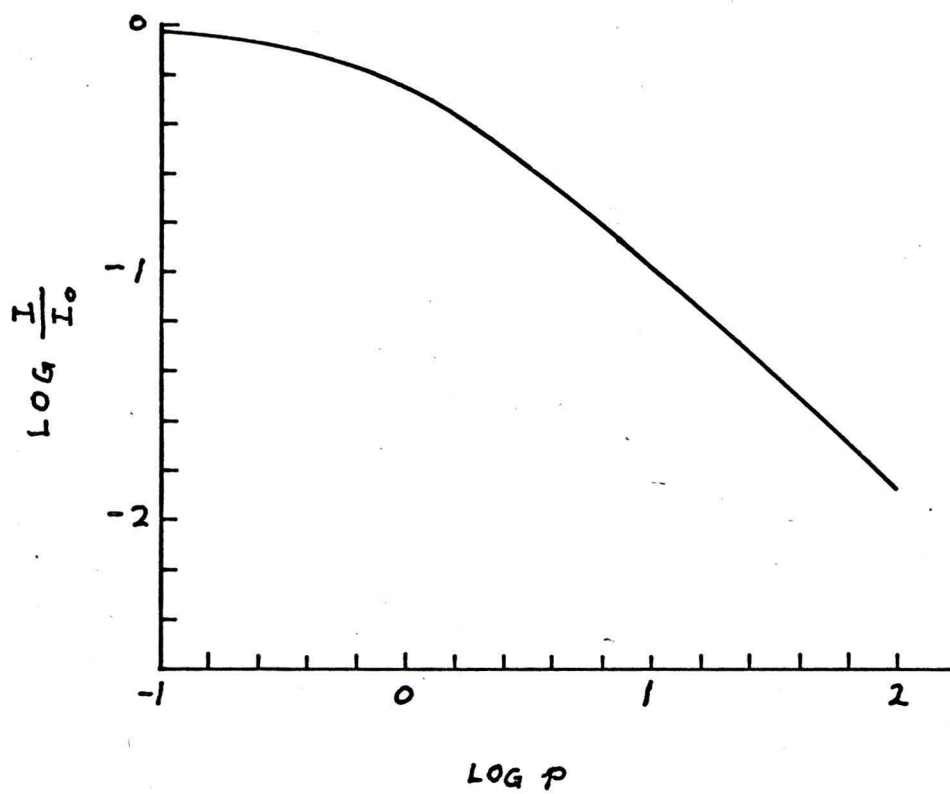


Figure 3. Reversal curve for Resonance line shape (after 55).

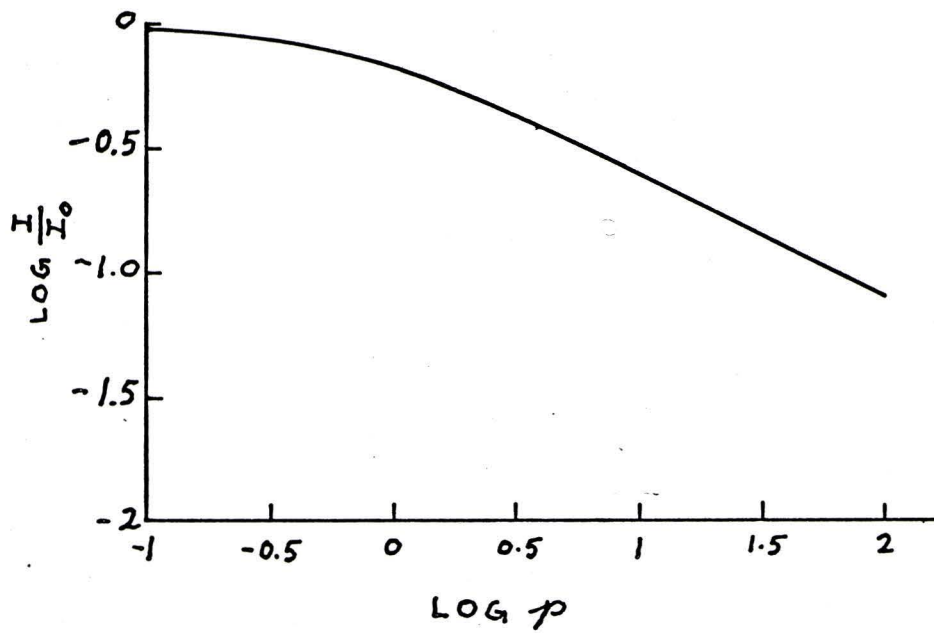


Figure 4. Reversal curve for Doppler Line Shape (after 55).

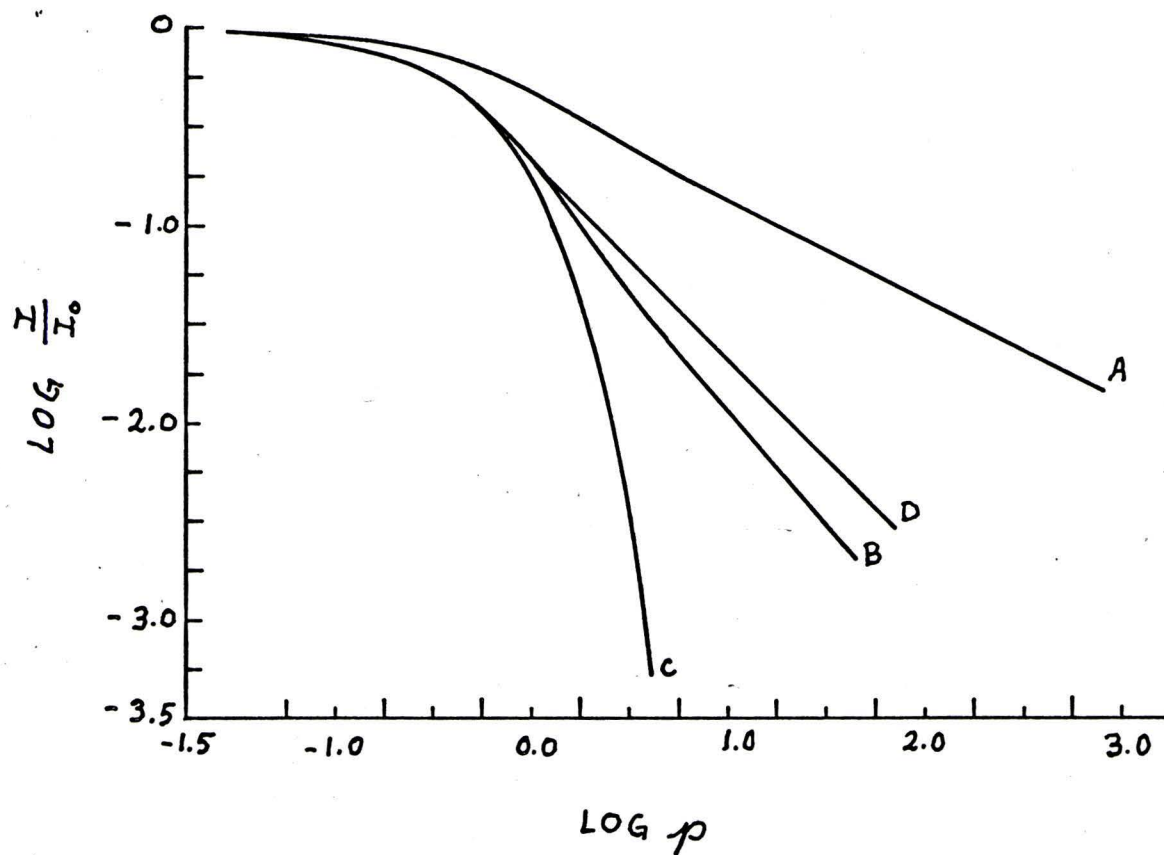


Figure 5. Calculated reversal curves obtained under different conditions of line shape and measurement. A: resonance shape; I is total intensity. B: same for Doppler shape. C: arbitrary shape; I is intensity at center of line. D: arbitrary shape; I is intensity at line maximum (after 55).

show a characteristic dip in intensity at the line center. This case is called "self reversal." It is possible to have self reversal in isothermal as well as nonisothermal sources.^{(7) (28) (26) (27)} The stark broadened lines of hydrogen show a central dip due to the absence of a central stark component which should not be confused with possible self reversal. When a central dip is not observed, it is not necessarily safe to conclude that self absorption effects are negligible. The profile of a line with 40 percent self absorption is almost indistinguishable from the unabsorbed profile except for the difference in integrated intensity. Thus the absence of self reversal is a necessary but by no means sufficient condition for disregarding self absorption.

Boltzmann Plot

If nothing is known about the temperature or density in a source, the first thing which is often done is to make a so-called Boltzmann graph. This is a plot of (essentially) intensity versus the excitation energy of the upper level. In making this plot the following assumptions are made about the source in question:

- 1) thermodynamic equilibrium
- 2) optical thinness

(these requirements will be relaxed later). In particular, what is required is a Boltzmann distribution of particles in the various energy states and a source isothermal to the extent that it makes sense to speak of an "average" temperature.⁽⁵⁸⁾

Using the equation for the intensity of an optically thin line,

$$\textcircled{1} \quad I = \frac{2hc}{\lambda^3} \frac{\pi e^2}{mc} \frac{g_u f_{ul}}{U(T)} N_0 \exp\left[-\frac{E_u}{kT_e}\right],$$

where

$$N_0 = \int n(r) dr .$$

Multiplying 1 by $\frac{\lambda^3}{g_u f_{ul}}$, taking common logarithms of both sides and converting E_u from ergs to eV gives

$$\overbrace{\log \frac{I \lambda^3}{g_u f_{ul}}}^y = \overbrace{\left(-\frac{5040}{T_e}\right)}^m E_u^x + \overbrace{\log \left(\frac{2h\pi e^2}{m} \frac{N_0}{U(\tau)}\right)}^b,$$

giving the equation for a straight line

$$y = mx + b$$

Thus in a plot of y versus x , i.e. $\log \frac{I \lambda^3}{g_u f_{ul}}$ vs. E_u the slope of the (hopefully) straight line will be $-\frac{5040}{T_e}$ thereby yielding T_e , and the y intercept ($E_u = 0$) gives

$$\log \frac{I \lambda^3}{g_u f_{ul}} = \log \frac{2h\pi e^2}{m} \frac{N_0}{U(\tau)},$$

or

$$N_0 = \frac{I \lambda^3 m U(\tau)}{2\pi h e^2 g_u f_{ul}},$$

yielding N_0 if I has been measured in absolute units. We now ask what the effects will be of relaxing assumptions 1 and 2.

If a temperature gradient exists in the source but the energy distribution at any one point is still Boltzmann (referred to as local thermal equilibrium), model atmospheres for the source can be constructed to see how the Boltzmann plot is affected. Hefferlin⁽³⁷⁾ has done this for an atmospheric arc by assuming families of curves for $T_e(r)$ and $n_0(r)$. He examined 20 models,

$$T_e(r) = T_e(0) \exp\left[-\frac{r^2}{p^2}\right] + 300$$

$$p = 1, 2, 3, 4, 5, 6$$

$$\left(\frac{n_0(r)}{n_0(0)}\right)^m + \left(\frac{r}{R}\right)^m = 1$$

$$m = \frac{1}{3}, \frac{1}{2}, 1, 2, 3$$

$$T_e(0) = 5300^\circ K$$

$$n_0(0) = 10^{16} \text{ atoms cm}^{-3}$$

and computed the intensities of the lines arising from each energy level E_i of an imaginary atomic species in the arc. Boltzmann graphs were plotted for each model. All the resulting curves were linear yielding a value for \bar{T}_e very near the central value.

$$[T_e(o) - \bar{T}_e \doteq 50^\circ K \pm 20^\circ K]$$

This rather unexpected (though welcome) result is due to the decrease in both T and n causing a drastic reduction in the ability of the gas to radiate and is vital for our next consideration.

We consider now the effect of finite optical depth, i.e. what will self absorption do to the points on the graph? Self absorption causes I the observed intensity, to be less than the optically thin intensity for the same excitation conditions. Thus the effect of self absorption is to drive the points toward smaller "y" values. However, since the lower excitation levels are more subject to self absorption, the upper levels appear overpopulated with respect to the ground state; the net effect is to give values of \bar{T}_e which are too high. What is necessary then is to draw a curve representing the true \bar{T}_e and N_o of the source and ascribe the vertical scatter to self absorption. Unfortunately, it is usually just this \bar{T}_e and N_o which is being sought in making a Boltzmann graph. What is usually done is to draw an envelope above and to the right of the data points, (37) perform an iteration, (52) and ascribe the remaining vertical scatter to self absorption. This method must be used with care, however, for other factors may also induce vertical scatter such as errors in intensity measurements.

Blackbody Ceiling

Comparing the absolute intensity of a spectrum line with the

intensity of the blackbody ceiling (value of B_λ) at the same wavelength and same excitation temperature gives information about possible self absorption. (59) As the intensity of a line approaches the blackbody ceiling, it is said to saturate, the optical depth becomes infinite, and the source radiates at that wavelength with the intensity given by the Planck function. Another way of saying the same thing is that when the intensity has reached the blackbody ceiling, adding more atoms (increasing the concentration) causes no further increase in intensity because (due to the infinite optical depth) none of the photons given off by the additional atoms will ever leave the source but will all be reabsorbed.

It should be noted that nonresonance lines in laboratory sources are usually several orders of magnitude less than the blackbody ceiling. Therefore, if the specific intensity of the line is near the blackbody ceiling at the same wavelength and excitation temperature, the line may be saturating and should be examined with special care.

SECTION IV

USING SELF ABSORPTION TO DETERMINE ABUNDANCE AND LINE SHAPE PARAMETER a

Self absorption may be used to determine abundances for resonance lines with fairly high oscillator strengths.⁽⁴⁷⁾ ⁽⁵⁶⁾ There is, however, no restriction with respect to temperature and wavelength. In order to calculate abundance it is necessary to know the Doppler width, the oscillator strength, and the physical path length, l . Self absorption measurements also allow calculation of the "a parameter," the ratio of damping to Doppler broadening.⁽⁵⁶⁾

Method Based on the Shape of the "Curve of Growth"

The double-logarithmic plot of the intensity of the line as a function of the concentration C , is called the "experimental curve of growth." This curve shows a typical convex curvature due to self absorption and is characterized by the positions of its initial and final asymptotes of $C \rightarrow 0$ and $C \rightarrow \infty$ respectively. The experimental curve of growth should be superposable on one of the "theoretic curves of growth" by a shift parallel to both axes of plotting. The theoretic curve of growth is a plot of χ_y vs. w_y . The theoretic curve is completely determined by the a-parameter. The a-parameter is a function of the particular kind of atom, the line considered, the temperature, the plasma composition, and the pressure. From the superposition of the experimental curve on one of the theoretic, the value of the a-parameter and the atomic abundance in the plasma can be derived.

The theoretic curve of growth has two asymptotes given by⁽³³⁾ (34)

$$Y = \frac{\pi e^2}{m c} \gamma_\nu \quad \text{when} \quad \gamma_\nu \rightarrow 0$$

$$Y = \left\{ \frac{2\pi^2 e^2}{m c} \gamma a \right\}^{1/2} \quad \text{when} \quad \gamma_\nu \rightarrow \infty .$$

The ordinate of the intersection point, Y_s , is given by⁽³³⁾ (34)

$$Y_s = 2a .$$

The accuracy of this method in determining the a-parameter is about 8-10 percent. Figure 6 clearly shows that the determination of the a-parameter can be successful only for a-values of the order of 1. In this case the shape of the curve of growth in the region between the corresponding curves of growth are mutually very similar in shape and an accurate determination of the a-parameter fails in this case.

Method Based on the Duplication Curve

According to the definition, the theoretic duplication curves (i.e. D as a function of concentration in the plasma) may be calculated from the corresponding curve of growth for a certain value of the a-parameter.

The "experimental duplication curve" can be obtained by plotting (double-logarithmically) the D factor measured for a resonance line as a function of the concentration, corrected for reflection losses. The D-curve is in principle a differentiated curve of growth and has two horizontal asymptotes, namely, the initial asymptote: $D = 1.00$ and the final asymptote: $D = 2^{\frac{1}{2}} - 1 = 0.415$. For values of the a-parameter lower than 1.0, the D-curve shows a typical minimum (Figure 7). The experimental D-curve should be superposable on one of the (double-logarithmic) theoretic D-curves by a shift parallel to both axes of plotting. The D-factor has then only to be known in relative

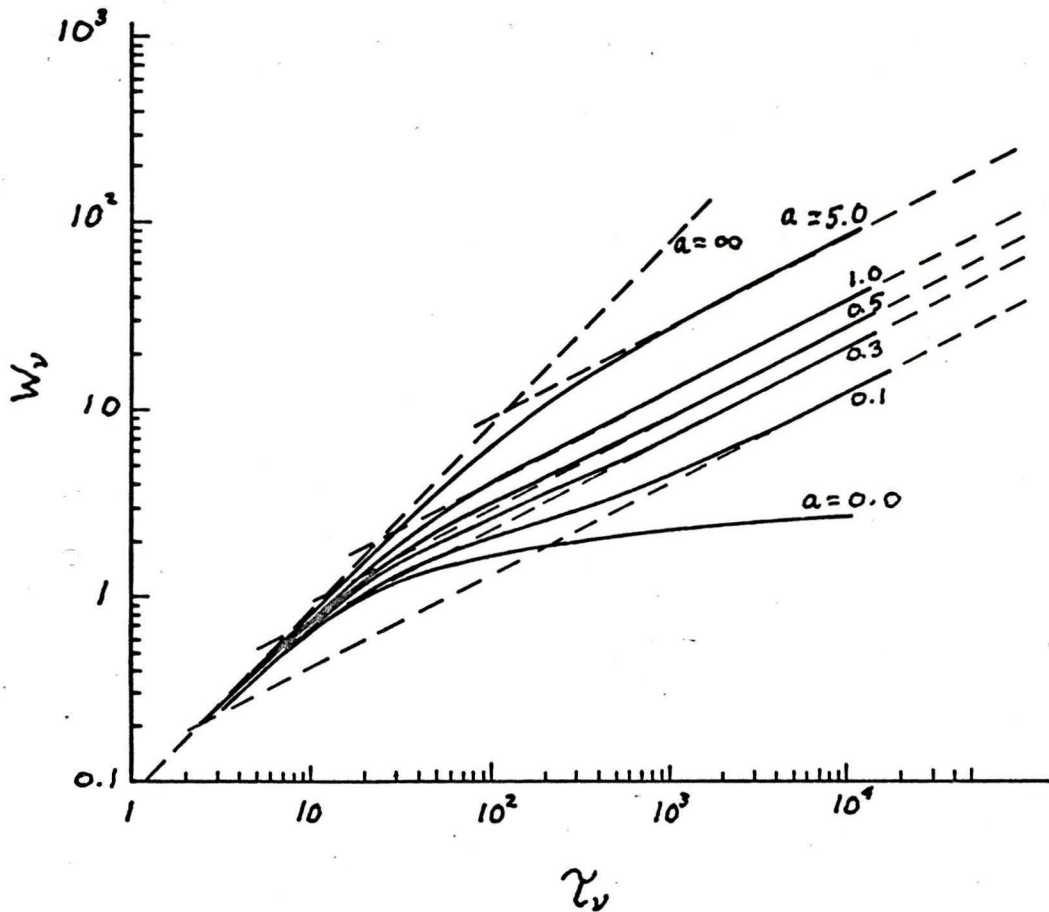


Figure 6. Some theoretic curves of growth for a single spectral line for a-parameter values ranging from 0.0 to 5.0 (after 56).

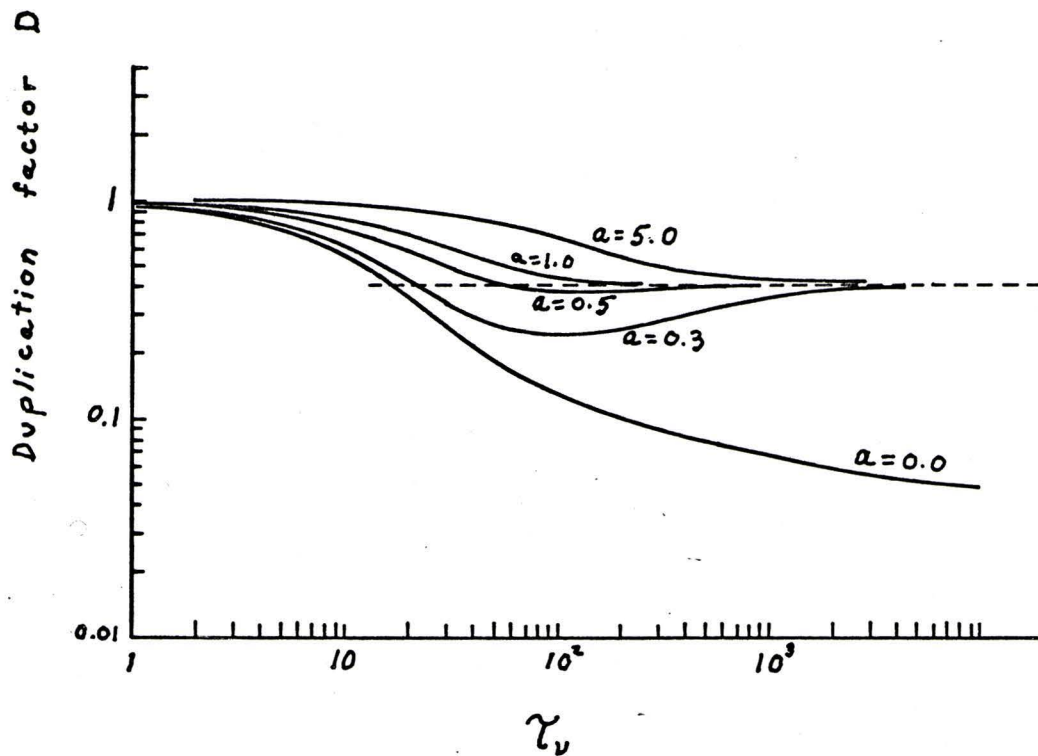


Figure 7. Some theoretic duplication curves for a single spectral line for a -parameter values in the range of 0.0 - 5.0 (after 56).

measure. From this comparison the value of the relevant a-parameter and that of the atomic content of the plasma may be derived.

If the relevant a-parameter is known this method yields the actual atomic content. An advantage of this method is, that it yields the correct concentration also in the case that the curve of growth would be distorted by ionization. The derivation of the a-parameter in the above way is not always accurate, however. In the range of a-values where the D-curve has a minimum, we may obtain a rather accurate a-parameter value from the depth of the minimum with respect to the final asymptote. However, if $a \geq 1$, the method fails since the minimum disappears. For the application of the above method a large number of theoretic D-curves (for a-parameter values in the range 0.5.0) has to be available. A genuine advantage is, however, that only relative intensity measurements are necessary. (62)

The duplication curves show a minimum value in the finite region for $a \leq 1$. The smaller the a-parameter value concerned, the deeper the minimum of the corresponding D-curve. For $a > 1$ the D-curves have no minimum point.

Method Combining the Curve of Growth with the Duplication Curve (56)

The value of the a-parameter and of the atomic concentration may be found by measuring simultaneously the experimental curve of growth and D-curve. The D-factors measured have to be converted into absolute values by correcting for losses at the reflection.

In the experimental curve of growth the ordinate of the point of intersection of the two asymptotes is determined in relative measure. Denote this point by y_s . For several abundances in the environment of the concentration corresponding to the intersection point, the ordinates

y_i are read from the experimental curve of growth. The corresponding D-factors are also experimentally determined. Denote these by D_i . From the theoretic curve of growth with a certain a-parameter the abscissa value (= N, apart from a constant factor) is derived, which belongs to a theoretic value Y_i , for which holds: $Y_i/Y_s = y_i/y_s$ (where Y_s is the ordinate of the intersection point of the asymptotes of the theoretic curve of growth concerned). This procedure is repeated for different values of the a-parameter. In a similar way the abscissa values corresponding to the measured values D_i are derived from the theoretic duplication curve, again for the different a-values. For each concentration considered we may construct now two (double-logarithmic) curves of a-parameter versus atomic concentration, which follows from the experimental value of y_i/y_s and D_i , respectively. The intersection point of both curves yields N for the relevant abundance and a (see Figure 8).

For this method the accurate determination of the experimental curve of growth, in particular, the relative position of its asymptotes is required. Furthermore, the experimental D-factors have to be known in absolute measure. For the application of this method we need theoretic curves of growth and duplication curves for a-parameter values ranging from 0 - 5.0.

It should be noted, however, that only relative intensity measurements have to be made. Calibration with a background source or knowledge of the properties of monochromator, filters, etc. are not required. The above procedure may be repeated for different abundances. This provides an internal check on the determination of the a-parameter (which should be relatively independent of abundance) and on the determination of N (which should be proportional to the abundance).

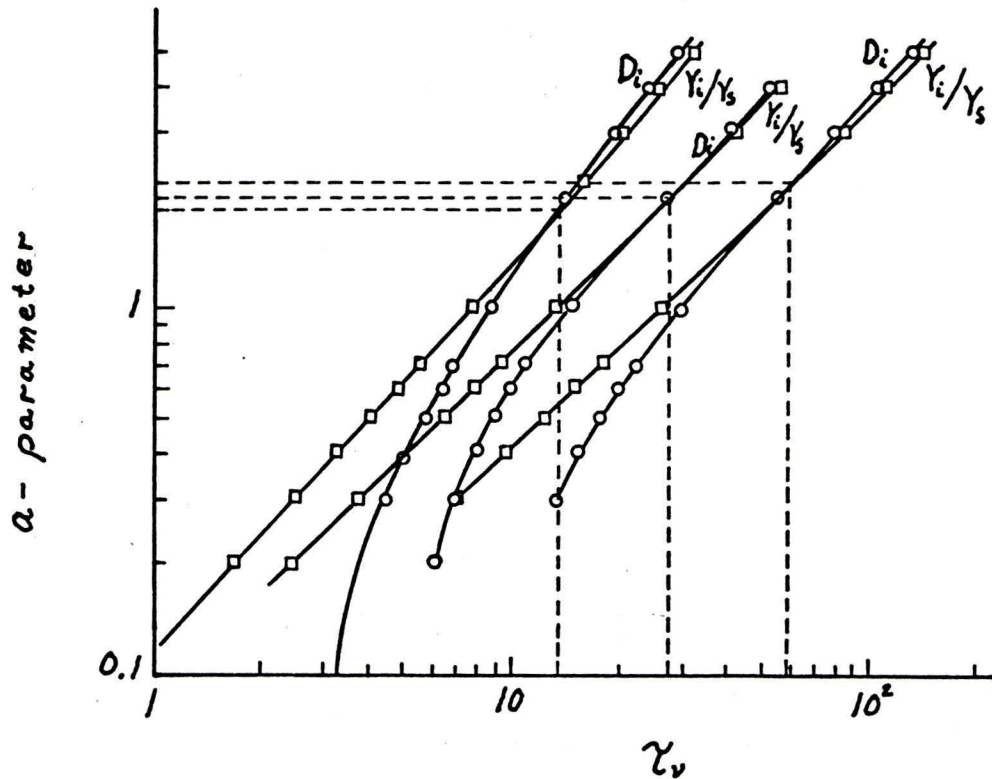


Figure 8. Graphical interpolation procedure for deriving the a-parameter and the absolute abundance N , by combining the curve of growth with the duplication curve (after 56).

Figure 8 illustrates the graphical interpolation procedure for deriving the a-parameter and the absolute abundance N, by combining the curve of growth with the duplication curve. For three abundances plots are given that relate the assumed (yet unknown) a-parameter to the abundance N in the flame as derived with this a-value from, on the one hand, the curve of growth and the relative emission values measured (Y_i/Y_s) and from the duplication curve and duplication factors measured (D_i), on the other.

The intersection of both plots should yield the true a-parameter of the line in question and the true atomic abundance.

SECTION V

EXPERIMENTAL DETERMINATIONS OF SELF ABSORPTION IN A PLASMA JET

In an attempt to compare various optical thickness tests with experiment, data was taken by Hefferlin⁽⁵⁹⁾ on a D.C. plasma jet operating with Mn seeded argon gas in the laminar mode at atmospheric pressure. The plume was studied at the nozzle and one inch downstream. Absolute intensities were measured and compared to the intensity of the blackbody ceiling and also to the optically thin intensity allowing calculation of the integrated optical depth parameter p . The raw data is given along with details of the calculation of the p parameter, and blackbody ceiling comparison.

At the nozzle of the plasma jet ($z = 0$), the optical thinness was tested in the following ways: (Figure 9)

A Boltzmann plot was constructed giving the following results:

MnI: optically thin because points fell in straight line as shown on Figure 10.

MnII: optically thin because points fell in straight line as shown on Figure 10.

All other species were ambiguous due to too few points or not enough spread along the E_u axis.

The integrated optical depth parameter p was calculated (see calculations in Table I):

HI: 40% of optically thin intensity expected.

NI: $(10^{13} \text{ cm}^{-2})$ 18% of optically thin intensity expected.

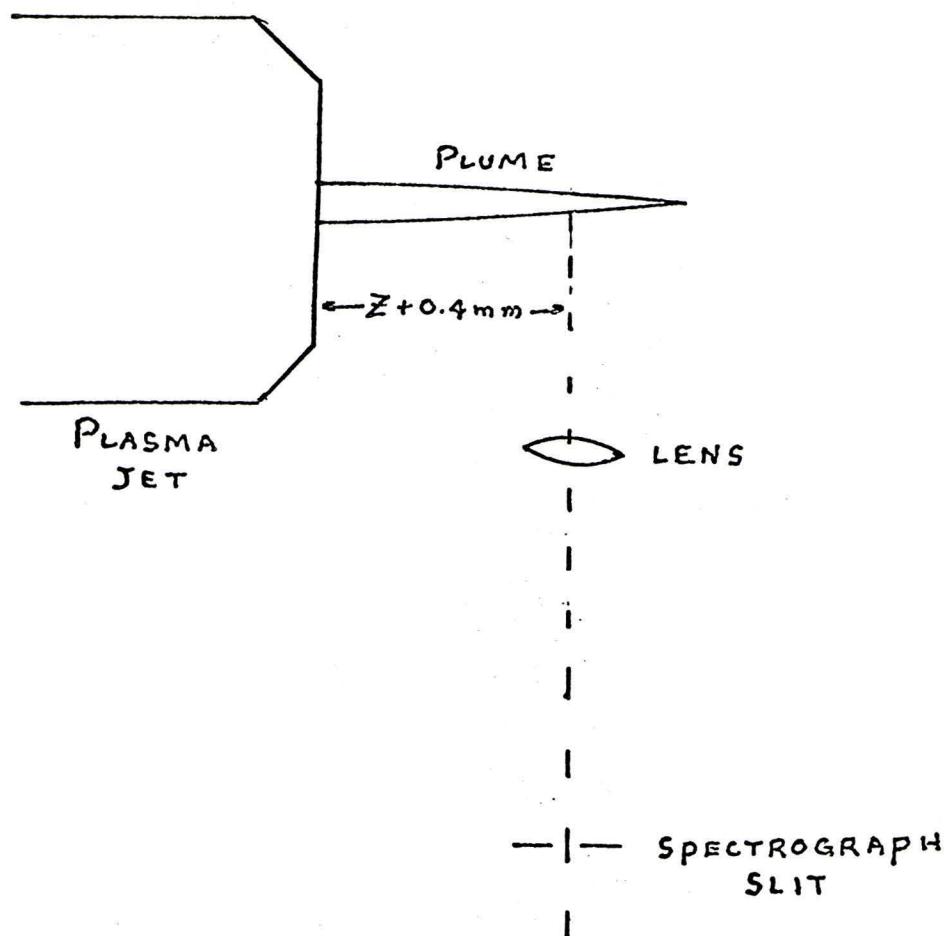
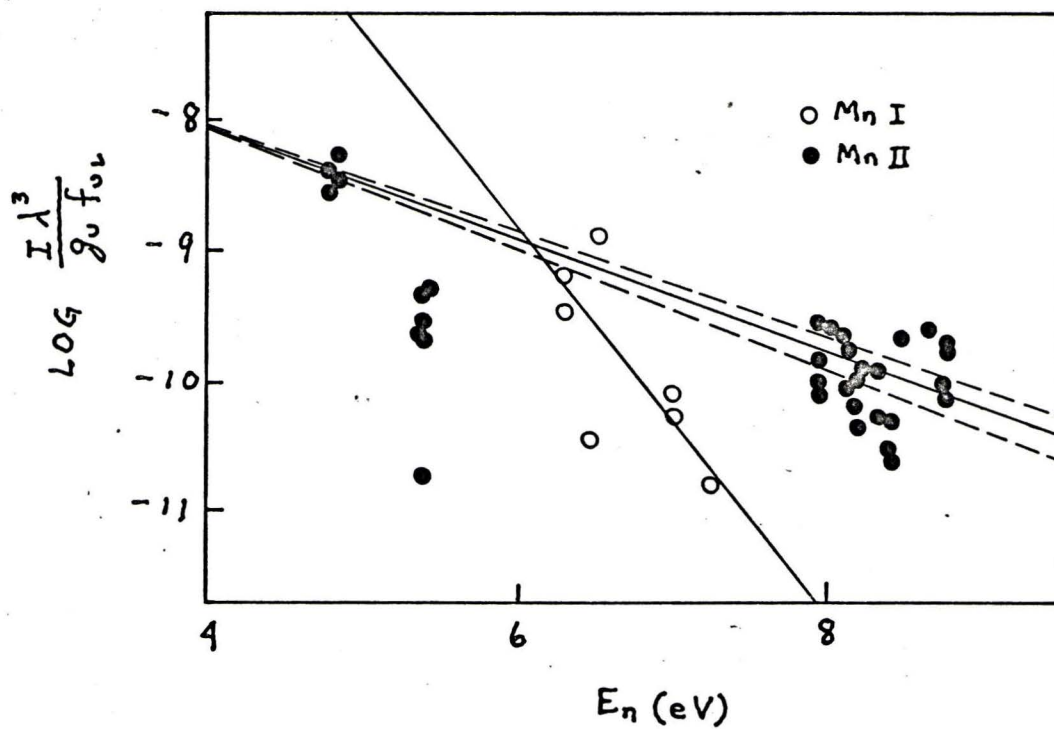


Figure 9. The Plasma Jet and Optical System



- NI: $(10^{16} \text{ cm}^{-2})$ heavy self reversal.
 ArI: no measurable self absorption.
 ArII: 56% of optically thin intensity expected.
 MnI: 80% of optically thin intensity expected
 (3,000°K or 12,000°K).
 MnII: no measurable self absorption.

Comparing absolute specific intensity of a line with that of the Planck function at the same wavelength and excitation temperature gave the following (see calculations in Table II):

No measurable self absorption except for MnI and then only if lower temperature obtained.

Observing the line profile showed that:

The ArI line at 7635A reported reversed under similar conditions by Olsen⁽⁶⁰⁾ was scanned and photographed under sufficiently high resolution that the absence of significant "dip" was certain.

One inch down the flow stream ($Z = 1''$), the optical thinness was tested in the following ways:

Boltzmann plot:

N_2^+ : optically thin because the points fell in a straight line. No other species had enough measurable lines.

Integrated optical depth parameter p (see calculations in Table III):

- HI: no measurable self absorption.
 ArI: 80% of the optically thin intensity expected.
 ArII: no measurable self absorption.
 MnI: no measurable self absorption.

Comparing the absolute specific intensity of a line with that of

the Planck function at the same wavelength and excitation temperature (see calculation in Table IV):

no measurable self absorption for any species.

As can be seen, the self reversal parameter p , tends to be over-conservative by about an order of magnitude compared with other self absorption tests. Since this test is such a strong function of source model, an effort is being made⁽⁵⁴⁾ to calculate this parameter for various alternative models.

TABLE I

Details of Calculations for
Self Reversal Parameter p , at $Z = 0$

	H I	NI	H I
$\lambda(\text{Å})^*$	4500	4500	4500
$\Delta\lambda(\text{cm})^*$	11×10^{-8}	1×10^{-8}	1×10^{-8}
$gf^{*\dagger}$	10^1	3	3
$N_0(\text{cm}^{-2})^*$	10^{14}	$10^{13\#}$	$10^{16\#}$
$E_L(\text{ev})$	10.0	10.0	10.0
$T_e(^{\circ}\text{K})^*$	12,000	12,000	12,000
$\log p$	0.486	1.005	4.005
$\log I/I_0\%$	-0.4	-0.8	Large
Self absorbed? [ⓐ]	↓	↓	↓
Self reversed? [ⓐ]	Some	Yes	Heavily

$$p = \frac{e^2}{mc} \frac{1}{\Delta\nu} \frac{g_u f_{ul}}{g_o} N_u \exp[-E_L/kT_e]$$

TABLE I (Continued)

Ar I	Ar II	Mn I	Mn II
4500	4500	4500	4500
3×10^{-8}	1×10^{-8}	1×10^{-8}	1×10^{-8}
10^{-2}	10^0	10^0	10^1
10^{17}	10^{17}	10^{13}	10^{13}
11.8	17.0	0.0^+	3.0
12,000	12,000	Any ⁺	12,000
-1.383	0.252	-0.650	-1.196
0.0	-0.2	-0.1	0.0
No	No	No	No
No	Very Little	No	NO

* approximate because chosen before experimental data were all in and/or done for typical case.

⁺ not a function of temperature since exponential becomes unity for $E_1 = 0$.

[†] also assumed $g_0 = 1.0$, $g_1 = 4.0$.

[‡] Cowan and Dieke (1948) p. 434. (55)

[@] Cowan and Dieke (1948) p. 401. (55)

TABLE II

Details of the Calculations to Compare Line Center Specific Intensity with Planck Function at Same Wavelength. Lines Selected were the Most Intense and/or Illustrated Typical Lines in a Given Spectral Region. $Z = 0$.

Specie	Line Wave- Length (A)	I_{λ} (erg/sec ster cm^2cm)	T ($^{\circ}\text{K}$)*	$B_{\lambda}(T)$ (erg/sec ster cm^2cm)
H I	6562	3.78×10^{12}	12,000	1.90×10^{15}
	4861	4.94×10^{11}	12,000	4.10×10^{15}
Ar I	4158	3.51×10^{12}	12,000	5.84×10^{15}
	4272	9.14×10^{11}	12,000	5.44×10^{15}
	4345	3.68×10^{11}	12,000	5.25×10^{15}
Ar II	4426	1.97×10^{12}	12,000	5.03×10^{15}
	4879	8.86×10^{11}	12,000	4.06×10^{15}
Mn I	2836	3.68×10^{12}	12,000	7.70×10^{16}
			3,000	2.81×10^{10}
	2830	1.51×10^{12}	12,000	9.49×10^{15}
			3,000	2.79×10^{10}
Mn II	2892	3.24×10^{12}	12,000	9.36×10^{15}
	2933	5.86×10^{12}	12,000	9.29×10^{15}

* Estimated, ahead of final results, as average temperature through a diameter at $Z = 0$.

TABLE III

Details of Calculations for
Self Reversal Parameter p , at $Z = 1$ "

	H I	N I	Ar I	Ar II	Mn I	Mn I
$\lambda(\text{A})^*$	4500	4500	4500	4500	4500	4500
$\Delta\lambda(\text{cm})^*$	11×10^{-8}	11×10^{-8}	3×10^{-8}	1×10^{-8}	1×10^{-8}	1×10^{-8}
gf^{\dagger}	10^1	10^1	10^{-2}	10^0	10^1	10^0
$N_0(\text{cm}^{-2})^*$	10^{13}	10^{10}	10^{17}	10^{15}	10^{11}	10^8
$E_i(\text{ev})$	10.0	10.0	11.8	17.0	0.0^+	0.0^+
$T(^{\circ}\text{K})^*$	9.500	9,500	9,500	9,500	Any ⁺	Any ⁺
$\log p$	-2.194	-5.194	-0.039	-2.750	-2.848	-5.828
$\log I/I_0^{\%}$	0.0	0.0	-0.1	0.0	0.0	0.0
Self absorbed? [ⓐ]	No	No	Very little	No	No	No
Self reversed? [ⓐ]	No	No	No	No	No	No

$$p = \frac{e^2}{mc} \frac{1}{\Delta\nu} \frac{g_u f_{ul}}{g_l} N_0 \exp[-E_l/kT_0]$$

* approximate because chosen before experimental data were all in and/or done for typical case.

⁺ not a function of temperature since exponential becomes unity for $E_l = 0$.

[†] also assumed $g_l/g_u = 1.0$, $g_0 = 4.0$.

[Ⓢ] Cowan and Dieke (1948) p.434. (55)

[ⓐ] Cowan and Dieke (1948) p. 421. (55)

TABLE IV

Details of the Calculations to Compare Line Center Specific Intensity with Planck Function at same Wavelength. Lines Selected were the most Intense and/or Illustrated Typical Lines in a given Spectral region. $Z = 1''$.

<u>Specie</u>	<u>Line Wave- Length (A)</u>	<u>I_{λ} (erg/sec ster cm^2cm)</u>	<u>T ($^{\circ}\text{K}$)*</u>	<u>$B_{\lambda}(T)$ (erg/sec ster cm^2cm)</u>
Ar II	4806	1.21×10^1	9,000	1.72×10^{15}
	4880	6.02×10^1	9,000	1.69×10^{15}
Mn I	4033	1.36×10^2	9,000	2.16×10^{15}
	4052	5.9×10^0	9,000	2.15×10^{15}

* Estimated, ahead of final results, as average temperature through diameter at $Z = 1''$.

TABLE V

Spectral Line Intensities (ergs sec⁻¹ ster⁻¹ cm⁻²)

Specie	Line A	log gf	Z = 0		Z = 1"	
			Intensity	FWHM A	Intensity	FWHM A
H I	α	+0.71	5.8×10^5	12.0		
	β	-0.02	3.3×10^5	48.0		
	γ	-0.45	2.8×10^5	86.0		
Ar I	4158.59	-1.841	1.2×10^5	2.8		
	4164.18	-2.771	9.1×10^4	3.8		
	4181.88	-2.491	2.0×10^4	4.0		
	4200.68	-1.862	9.6×10^3	2.8		
	4259.36	-2.051	4.5×10^3	3.8		
	4266.29	-2.425	3.5×10^4	3.8		
	4272.17	-2.309	3.3×10^3	3.0		
	4300.10	-2.327	3.3×10^3	3.0		
	4345.17	-2.620	4.5×10^3	1.0		
	4510.73	-2.517	2.1×10^4	4.8		
Ar II	5062.07	-0.508	1.7×10^3	1.1		
	5009.35	-0.558	2.1×10^3	1.0		
	4879.90	-0.215	3.3×10^3	1.0		
	4847.07	-1.172			60.0	2.0
	4806.07	+0.082	1.2×10^4	1.0	11.0	0.9
	4764.90	-0.329	3.3×10^3	1.0	12.0	1.0
	4609.60	+0.367	3.3×10^3	0.9	4.2	0.6
	4589.93	+0.070	2.1×10^3	1.2		
	4579.39	-0.326	4.5×10^4	1.0		
	4426.01	+0.450	9.3×10^3	0.9		

TABLE V (Continued)

Specie	Line A	log gf	Z = 0		Z = 1"	
			Intensity	FWHM A	Intensity	FWHM A
	4379.74	-0.172	7.6×10^3	1.0		
	4013.87	-0.328	3.3×10^3	0.9		
Mn I	4055.21	+0.31			7.2	0.9
	4052.47	+2.40			5.9	1.0
	4048.76	+0.12			7.2	1.0
	4041.36	+0.60			15.0	1.0
	4034.49	-0.79			101.0	1.0
	4033.07	-0.62			137.0	1.0
	3926.47	+ .50	3.5×10^3	0.9		
	3161.04	+ .06	2.2×10^4	1.2		
	3047.04	+ .68	2.3×10^3	1.0		
	2836.31	- .50	1.7×10^4	1.0		
	2830.79	- .05	1.3×10^9	1.0		
Mn II	3488.78	0.24	1.3×10^3	0.8		
	3482.91	0.43	1.2×10^3	0.7		
	3474.04	0.51	2.5×10^3	1.0		
	3460.33	0.52	2.5×10^3	0.8		
	3441.99	0.80	4.8×10^3	0.7		
	2949.20	0.94	9.1×10^4	0.7	578.0	1.0
	2939.30	0.84	6.8×10^4	0.7	616.0	0.6
	2933.06	0.72	3.8×10^4	0.6	368.0	0.6
	2892.39	0.70	2.3×10^4	0.7		
	2889.58	1.15	8.1×10^3	0.7		
	2879.49	0.84	8.0×10^3	0.7		
N ₂ ⁺	0-0 sequence		1.3×10^5		6.38×10^3	

GLOSSARY

- a — natural damping ratio, the ratio of the natural breadth to the Doppler breadth $= \frac{\Delta \nu_L}{\Delta \nu_D} (\ln 2)^{1/2}$.
- A_{ul} — the Einstein coefficient of spontaneous emission (sec^{-1}).
- B_ν — Planck blackbody function ($\text{erg cm}^{-2} \text{cps}^{-1}$)

$$= \frac{2h\nu^3}{c^2} \frac{1}{e^{h\nu/kT_e} - 1}$$
- B_{lu} — Einstein coefficient of absorption ($\text{cm}^3 \text{erg}^{-1} \text{sec}^{-1}$).
- B_{ul} — Einstein coefficient of induced emission ($\text{cm}^3 \text{erg}^{-1} \text{sec}^{-1}$).
- D — duplication factor $= \frac{\Delta I}{I_0}$.
- E_l — lower energy level (ev).
- E_u — upper energy level (ev).
- $E_{(y)}$ — excitation parameter $= \frac{\bar{n}_u(r)}{\bar{n}_l(r)}$.
- f_{lu} — absorption oscillator strength.
- f_{ul} — emission oscillator strength.
- FWHM — full width at half maximum of a spectrum line (cps).
- g_0 — statistical weight of the ground state.
- g_l — statistical weight of the lower state.
- g_u — statistical weight of the upper state.
- HWHM — half width at half maximum of a spectrum line (cps).
- I — integrated intensity ($\text{ergs cm}^{-2} \text{ster}^{-1}$) $= \int I_\nu d\nu$.
- I_ν — specific intensity ($\text{ergs cm}^{-2} \text{cps}^{-1} \text{ster}^{-1}$).
- I_0 — specific intensity of an optically thin line ($\text{ergs cm}^{-2} \text{cps}^{-1} \text{ster}^{-1}$).
- \hat{I}_ν — specific intensity normalized to the blackbody ceiling.

$I_o(\nu_o)$ -value of the specific intensity of an optically thin line at the line center.

J_o — spectral density of the continuous background radiation.

Assumed constant over the absorption line width.

(ergs cm^{-2} ster $^{-1}$)

J_y — source function; the ratio of emission to absorption coefficient (ergs cm^{-2} cps $^{-1}$ ster $^{-1}$).

k — Boltzmann's constant = 1.38×10^{-16} erg deg $^{-1}$.

k_y — mass absorption coefficient (cm^{-1}).

$^{\circ}\text{K}$ — degrees Kelvin.

l — physical path length (cm).

LTE local thermal equilibrium--occurs when the energy distribution at a point is described by the Maxwell-Boltzmann relation.

m — electron mass = 9.108×10^{-28} g.

M — atomic mass (g).

N — number density.

p — integrated optical thickness parameter.

P_y — line shape parameter (profile) (cps $^{-1}$).

$\bar{P}_a(\nu_o)$ -value of the absorption line shape parameter at the center of the line, averaged through the source.

$P_a(\nu, x)$ -absorption line shape parameter (profile) as a function of position (cps $^{-1}$ cm $^{-1}$).

r — distance from axis.

T — gas kinetic temperature ($^{\circ}\text{K}$).

T_e — electron excitation temperature ($^{\circ}\text{K}$).

\bar{T}_e — electron excitation temperature averaged over the optical path.

$U(T)$ — partition function.

u — distance from line center (cps) = $\nu - \nu_0$

W_ν — equivalent width (cps) = $\int \frac{I_0 - I_\nu}{I_0} d\nu$

x — distance along optic axis (cm).

y_1 — the ordinate of the experimental curve of growth for an abundance near that corresponding to the intersection point of the asymptotes.

y_s — the ordinate of the point of intersection of the asymptotes of the experimental curve of growth.

Y_1 — the ordinate of the theoretic curve of growth for a value of τ_ν near that corresponding to the intersection point of the asymptotes.

Y_s — the ordinate of the intersection point of the asymptotes of the theoretic curve of growth.

y — number density of atoms exterior to r capable of absorbing the line = $\int_r^{+\infty} \bar{n}_L(x) dx$

δ — damping constant.

δ — Doppler width.

$\Delta\nu$ — an increment of frequency (cps).

$\Delta\lambda$ — an increment of wavelength (cm).

$\Delta\nu_D$ — the Doppler breadth (cps) = $\frac{\nu_0}{c} \left\{ \frac{8kT}{M} \right\}^{1/2} (\ln 2)^{1/2}$

$\Delta\nu_L$ — the natural breadth (cps) = $A_{ul} / 2\pi$

ρ_ν — the radiation density.

τ_ν — optical depth = $k_\nu n_L l$

μ — = $\rho \frac{P(u)}{P(0)}$

Ω — solid angle.

APPENDICES

APPENDIX I

Consider absorption from a continuum where ρ is essentially constant over the line.

The time rate of absorption is

$$\frac{dE}{dt} = -c k \int_{\text{LINE}} P_a(\nu, x) \rho dx .$$

By definition,

$$\frac{dE}{dt} = n_L(x) B_{LU} \rho h\nu_0$$

where $N_1(x)$ is the density of atoms capable of absorbing the line.

Since we assume that ρ is independent of ν and

$$\int_{\text{LINE}} P_a(\nu, x) d\nu = 1$$

thus

$$c k \rho = h\nu_0 B_{LU} n_L(x) \rho$$

or

$$k = \left(\frac{h\nu_0 B_{LU}}{c} \right) n_L(x) .$$

APPENDIX II

Derivation of an expression for the self absorption parameter p , for the case of a resonance profile in a source with cylindrical symmetry. (55)

$$1 \quad p = \frac{h \nu_0 B_{LU}}{c} \bar{P}_a(\nu_0) N_L$$

multiply by $\frac{N_U A_{UL}}{N_U A_{UL}}$

$$2 \quad p = \frac{B_{LU}}{A_{UL}} \frac{N_L P_a(\nu_0)}{N_U c} h \nu_0 A_{UL} N_U$$

$$3 \quad \frac{A_{UL}}{B_{UL}} = \frac{8\pi h \nu_0^3}{c^3} \quad \text{or} \quad \frac{A_{UL}}{B_{LU}} = \frac{g_L}{g_U} \frac{8\pi h \nu_0^3}{c^3}$$

$$4 \quad p = \frac{g_U c^3}{8\pi h \nu_0^3 g_L} \frac{N_L \bar{P}_a(\nu_0)}{N_U c} h \nu_0 A_{UL} N_U$$

5 Assuming that the shape of the absorption line is not a function of position

$$\left[\frac{1}{2} \int_{-\infty}^{+\infty} \bar{n}_L(x) dx \right] P_a(\nu_0) = \frac{1}{2} P_a(\nu_0) \frac{1}{N_L} \int_{-\infty}^{+\infty} n_L(x) dx$$

$$= P_a(\nu_0) \frac{1}{N_L} N_L$$

$$= P_a(\nu_0)$$

$$6 \quad P_\nu = \frac{\delta}{\pi} \frac{1}{(\nu - \nu_0)^2 + \delta^2}$$

assuming a resonance profile

as $\nu \rightarrow \nu_0$

$$P_{\nu_0} = \frac{1}{\pi \delta}$$

7 HWHM is at $\nu - \nu_0 = \delta$

$$8 \quad P = \frac{g_u}{g_L} \frac{c^3}{8\pi h \nu_0^3} \frac{N_L}{N_u} \frac{1}{c} \frac{1}{\pi \delta} h \nu_0 A_{ul} N_u$$

$$9 \quad P = \frac{g_u}{g_L} \frac{c^3}{8\pi h \nu_0^3} \left[\frac{N_L}{N_u} = \frac{g_L}{2g_u} e^{h\nu_0/kT_e} \right] \frac{1}{c} \frac{1}{\pi \delta} h \nu_0$$

$$\times \left[A_{ul} = \frac{8\pi^2 e^2 \nu_0^2}{m c^3} f_{ul} \right] N_u$$

$$N_L = \frac{1}{2} \int_{-\infty}^{+\infty} n_L(r) dr$$

$$N_u = \int_{-\infty}^{+\infty} n_u(r) dr$$

$$10 \quad P = \frac{2e^2 N_u g_u}{c(2\delta) m^2 u(T)} f_{ul} \exp[-E_L/kT_e]$$

$$11 \quad 2\delta = \text{FWHM} = \Delta\nu = \frac{c}{\lambda_0^2} \Delta\lambda$$

$$= \frac{c}{\lambda_0^2} (\text{FWHM})$$

$$12 \quad p = \frac{e^2}{mc} \frac{1}{\Delta \nu} \frac{g_u f_{ul}}{U(T)} N_u e^{-E_u/kT_e}$$

\uparrow
 $2S$

$$13 \quad p = \frac{e^2}{mc} \frac{1}{\Delta \nu} \frac{g_u f_{ul}}{g_o} N_u e^{-E_u/kT_e}$$

APPENDIX III

Define
$$N_L = \frac{1}{2} \int_{-\infty}^{+\infty} \eta_L(r) dr$$

$$N_U = \int_{-\infty}^{+\infty} \eta_U(r) dr$$

and
$$\bar{\eta}_L(r) = \frac{\eta_L(r)}{N_L}$$

$$\bar{\eta}_U(r) = \frac{\eta_U(r)}{N_U}$$

then let

$$\bar{P}_a(\nu) = \frac{1}{2} \int_{-\infty}^{+\infty} \bar{\eta}_L(x) P_a(\nu, x) dx$$

and

$$p = \left(\frac{h\nu_0 B_{LU}}{c} \right) \bar{P}_a(\nu_0) N_L .$$

From equation 2, Section III, we may write

$$I_\nu(r) = I_0 P_e(\nu, r_0) \exp \left[- \frac{h\nu_0 B_{LU}}{c} \int_{r_0}^r \eta_L(x) P_a(\nu, x) dx \right] .$$

It immediately follows that

$$I_\nu = I_0 \int_{-\infty}^{+\infty} \eta_U(r) P_e(\nu, r) \exp \left[- \frac{p}{\bar{P}_a(\nu_0)} \int \bar{\eta}_L(x) P_a(\nu, x) dx \right]$$

representing an average over the source.

Assuming again that $P_e(\nu, x) = P_e(\nu, x) = P_\nu$
and setting

$$u = \nu - \nu_0$$

$$P_\nu \longrightarrow P(u)$$

we get

$$I(u) = I_0 P(u) \int_{-\infty}^{+\infty} \bar{n}_\nu(r) \exp\left[-\tau \frac{P(u)}{P(0)} \int_r^{\infty} \bar{n}_\nu(x) dx\right] dr.$$

Defining

$$\mu(u) = \tau \frac{P(u)}{P(0)}$$

the absorbed shape function for the integrated density through the
whole source

$$y = \int_r^{\infty} \bar{n}_\nu(x) dx$$

and

$$E(y) = \frac{\bar{n}_\nu(r)}{\bar{n}_\nu(r)}$$

it follows that

$$I(u) = I_0 P(u) \int_0^2 E(y) \exp[-\mu(u)y] dy$$

where $P(u)$ specifies the line shape and $E(y)$ specifies the source
model.

BIBLIOGRAPHY

1. Sawyer, R. A., Experimental Spectroscopy (Prentice-Hall, Inc., New York, 1944).
2. Harrison, Lord and Loofbourow, Practical Spectroscopy (Prentice-Hall, New Jersey, 1948).
3. Aller, L. H., The Atmospheres of the Sun and Stars, 2nd Edit. (The Ronald Press, New York, 1963).
4. Chandrasekhar, S., Radiative Transfer (Dover Publications, New York, 1960).
5. Griem, H. R., Plasma Spectroscopy (McGraw-Hill Book Company, New York, 1964).
6. Thomas, R. N. and Athay, R. G., Physics of the Solar Chromosphere (Interscience Publishers, Inc., New York, 1961).
7. Oxenius, J., JQSRT 6, 65 (1966).
8. Oxenius, J., JQSRT 5, 771 (1965).
9. Wilson, R., JQSRT 2, 477 (1962).
10. Kalkofen, W., JQSRT 6, 633 (1966).
11. Bott, J. F., Phys. Fluids. 9, 1540 (1966).
12. Bardocz, A. and Voros, T., JQSRT 6, 775 (1966).
13. Kolb, A. C., JQSRT 3, 365 (1963).
14. Wilner, B., Acta Polytech. Scand. 41, 1 (1966).
15. Holstein, T., Phys. Rev. 72, 1212 (1947).
16. Holstein, T., Phys. Rev. 83, 1159 (1951).
17. Hefferlin, R., to be published, JQSRT (1969).
18. Thomas, R. N., Ap. J. 108, 142 (1948).
19. Thomas, R. N., Ap. J. 109, 500 (1949b).
20. Thomas, R. N., Ap. J. 115, 550 (1952).

21. Thomas, R. N., Ap. J. 111, 165 (1950).
22. Thomas, R. N., Ap. J. 109, 480 (1949a).
23. Thomas, R. N., Ap. J. 131, 429 (1960).
24. Thomas, R. N., Ap. J. 125, 260 (1957).
25. Jefferies, J. T., Ap. J. 132, 775 (1960).
26. Jefferies, J. T. and Thomas, R. N., Ap. J. 129, 401 (1959).
27. Jefferies, J. T. and Thomas, R. N., Ap. J. 131, 695 (1960).
28. Jefferies, J. T. and Thomas, R. N., Ap. J. 127, 667 (1958).
29. Jefferies, J. T. and White, O. R., Ap. J. 132, 767 (1960).
30. Thomas, R. N. and Zirker, J. B., Ap. J. 134, 733 (1961).
31. Athay, R. G. and Thomas, R. N., Ap. J. 124, 586 (1956).
32. Warwick, J. W., Ap. J. 119, 190 (1954).
33. Hinnov, E., JOSA 47, 151 (1957).
34. Hinnov, E. and Kohn, H., JOSA 47, 156 (1957).
35. Hofmann, F. W. and Kohn, H., JOSA 51, 512 (1961).
36. McGregor, W. K., "Spectroscopic Measurements in Plasmas," Fifth Biennial Gas Dynamic Symposium, American Institute of Aeronautics and Astronautics, Northwestern University (1963).
37. Hefferlin, R. and Gearhart, J., JQSRT 4, 9 (1964).
38. Preobrazhenskii, N. G., Ois 14, 342 (1963).
39. Fishman, I. S., Shaimanov, I. Sh., Ilin, G. G., Ois 15, 595 (1963).
40. Fishman, I. S., Ois 13, 630 (1962).
41. Preobrazhenskii, N. G., Ois 7, 173 (1959).
42. Podmoshenskii, I.V. and Shelemina, V.M., Ois 6, 531 (1959).
43. Ilin, G. G., Ois 16, 559 (1963).
44. Wrubel, M. H., Ap. J. 111, 157 (1949).
45. Wrubel, M. H., Ap. J. 109, 66 (1949).
46. Preobrazhenskii, N.G., Ois 17, 8 (1963).

47. Rukosueva, A. V., *OiS* 17, 340 (1936).
48. Ilin, G. G. and Fishman, I. S., *OiS* 20, 387 (1965).
49. Menzel, D. H., Baker, B. and Goldberg, L., *Ap. J.* 87, #2, 81 (1958).
50. Menzel, D. H., *Ap. J.* 84, 462 (1936).
51. Wrubel, M. H., *Ap. J.* 109, 66 (1948)
52. Letfus, V., *JOSA* 51, 1151 (1961).
53. Druzvesteyn, I. and Penning, V., *Rev. Mod. Phys.* 12, 87 (1940).
54. Hefferlin, R., private communication.
55. Cowan and Dieke, *Rev. Mod. Phys.* 20, 418 (1948).
56. Herrmann and Alkemade, *Photometry* (John Wiley & Sons, New York, 1966):
57. Alkemade, C., Thesis: Flame Photometry, University of Utrecht (1954).
58. Hefferlin, R., Progress in High Temperature Physics and Chemistry, Vol. 2 (Pergamon Press, Oxford, 1968), edited by C. A. Rouse.
59. Hefferlin, R., Progress in High Temperature Physics and Chemistry, Vol. 3 (Pergamon Press, Oxford, 1969), edited by C. A. Rouse.
60. Olsen, H. N., *JQSRT* 3, 305 (1963).
61. Bickel and Scoboria, *JQSRT* 5, 729 (1965).
62. Alkemade, C., Thesis: Flame Photometry, University of Utrecht (1954).

BIOGRAPHICAL SKETCH

George Robert Shipman was born January 3, 1944, in Bridgeport, Connecticut. He moved with his family to Orlando, Florida in 1953. He attended Fletcher Academy, Fletcher, North Carolina, and Forest Lake Academy, Maitland, Florida.

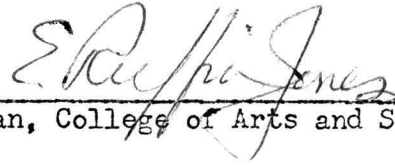
In 1961, he was enrolled at Southern Missionary College, Collegedale, Tennessee where he held a National Science Foundation Undergraduate Research Participantship. In September of 1962, he was enrolled at the University of Florida majoring in Physics. During 1963, he was employed by Jarrell-Ash Company, Newtonville, Massachusetts, and in 1964, he worked for Parametrics Inc. of Waltham, Massachusetts.

He re-enrolled at the University of Florida in September, 1964, and received the Bachelor of Science degree with a major in Physics in June, 1966, and was elected a member of Sigma Pi Sigma.

He was admitted to the Graduate School of the University of Florida in September of 1966 to pursue the Master of Science degree in Astronomy with a minor in Physics. He held a graduate assistantship with the Department of Physics.

This thesis was prepared under the direction of the chairman of the candidate's supervisory committee and has been approved by all members of that committee. It was submitted to the Dean of the College of Arts and Sciences and to the Graduate Council, and was approved as partial fulfillment of the requirements for the degree of Master of Science.

December, 1968



Dean, College of Arts and Sciences

Dean, Graduate School

Supervisory Committee:



Chairman

